# An aquaporin-4/transient receptor potential vanilloid 4 (AQP4/TRPV4) complex is essential for cell-volume control in astrocytes

Valentina Benfenati[a,1], Marco Caprini[b,1], Melania Dovizio[b], Maria N. Mylonakou[c], Stefano Ferroni[b], Ole P. Ottersen[c], and Mahmood Amiry-Moghaddam[c,2]

[a]Institute for Nanostructured Materials, Consiglio Nazionale delle Ricerche, 40129 Bologna, Italy; [b]Department of Human and General Physiology, University of Bologna, 40127 Bologna, Italy; and [c]Center for Molecular Biology and Neuroscience and Department of Anatomy, University of Oslo, 0317 Oslo, Norway

Edited* by Peter Agre, Johns Hopkins Malaria Research Institute, Baltimore, MD, and approved December 27, 2010 (received for review September 1, 2010)

**Regulatory volume decrease (RVD) is a key mechanism for volume control that serves to prevent detrimental swelling in response to hypo-osmotic stress. The molecular basis of RVD is not understood. Here we show that a complex containing aquaporin-4 (AQP4) and transient receptor potential vanilloid 4 (TRPV4) is essential for RVD in astrocytes. Astrocytes from AQP4-KO mice and astrocytes treated with TRPV4 siRNA fail to respond to hypotonic stress by increased intracellular $Ca^{2+}$ and RVD. Coimmunoprecipitation and immunohistochemistry analyses show that AQP4 and TRPV4 interact and colocalize. Functional analysis of an astrocyte-derived cell line expressing TRPV4 but not AQP4 shows that RVD and intracellular $Ca^{2+}$ response can be reconstituted by transfection with AQP4 but not with aquaporin-1. Our data indicate that astrocytes contain a TRPV4/AQP4 complex that constitutes a key element in the brain's volume homeostasis by acting as an osmosensor that couples osmotic stress to downstream signaling cascades.**

water channel | glia | brain edema

A basic property of any cell type is the ability to resist volume changes in the face of hypotonic stress. Thus, most cells are equipped with mechanisms that help bring cell volume back toward baseline level in the wake of an osmotically induced swelling response. This volume recovery, termed "regulatory volume decrease" (RVD) (1), plays a critical role in the brain, whose functional and structural integrity depends on finely tuned volume homeostasis at the cellular as well as the organ level.

A wealth of data indicates that astroglial cells are essential for the maintenance of volume homeostasis in brain (2). Being equipped with AQP4 water channels in their foot processes at the interface between brain and liquid spaces, astrocytes are the first cells to be exposed to osmotic changes and the first cells to swell in response to hypo-osmotic stress (3–5). Further, the proximity of the astroglial processes to the subarachnoidal space and vessels (which act as sinks for excess osmolytes) places astroglia in a unique position for mediating regulatory volume changes, on the part of the astrocytic syncytium and the brain as a whole.

A full mechanistic understanding of RVD would pave the way for more sophisticated measures to curtail pathological changes in brain water transport and distribution, as seen in brain tumors, stroke, and several other acute conditions that carry a high morbidity and lethality because of the loss of volume homeostasis. Future drugs affecting AQP4-mediated water transport would be expected to alleviate the acute consequences of inadvertent changes in osmotic driving forces. However, because the lipid bilayer of plasma membranes allows water diffusion (albeit to a restricted extent compared with membranes containing aquaporins), the long-term consequences of osmotic challenges can be offset only by manipulating the osmotic gradients per se. In this context, the RVD mechanisms stand out as targets of potential pharmacological interest (1, 6).

Previous studies of the molecular underpinning of RVD in astroglia have been concerned mainly with the effector mechanisms, most notably the properties of the volume-regulated anion channels (VRAC). Osmolyte efflux through VRAC is thought to provide the driving force for water exit (6, 7). The factors that initiate RVD have received comparatively little attention. Here we test our hypothesis that activation of astroglial RVD depends on a molecular interaction between AQP4 and TRPV4.

Our hypothesis rests on our recent finding that TRPV4 is strongly expressed in astrocytic endfeet membranes abutting the pia (including the extension of the pia that lines the Virchow–Robin spaces) and in endfeet underlying ependyma of the ventricular system (8). Thus, like AQP4, TRPV4 is expressed in membranes that provide access to the liquid spaces that act as sinks for excess osmolytes in the face of an osmotic challenge. In other tissues, TRPV4 is known to mediate $Ca^{2+}$ influx (assumed to act as a trigger of RVD) in response to osmotic stress (9–13). TRPV4 also is sensitive to membrane stretch and therefore is likely to be activated by water influx (14, 15). Thus, TRPV4 and AQP4 combined possess the essential features expected of an RVD activator.

Here we show that hypotonic stress initiates an increase in intracellular calcium ($[Ca^{2+}]_i$) and an RVD response in primary mouse astrocytes and that this response is absent in astrocytes from AQP4-KO mice and in WT astrocytes with siRNA-mediated TRPV4 knockdown. We also provide evidence that TRPV4 and AQP4 are coexpressed and interact in astrocytic plasma membranes in situ and in primary cultures, as well as in transfected cell lines. Using an astroglia-derived cell line that endogenously expresses TRPV4 but not AQP4, we show that hypotonic stress initiates an increase in $[Ca^{2+}]_i$ and an RVD response, but only if the cells are transfected with either isoform of AQP4 (3). We demonstrate that aquaporin-1 (AQP1), another member of the aquaporin family, cannot substitute for AQP4. Taken together our data indicate that AQP4 and TRPV4 are essential components of a molecular complex that is critically involved in the hypotonicity-induced rise in $[Ca^{2+}]_i$ and initiation of RVD in astrocytes.

## Results

Functional comparison of primary astrocytes from WT and AQP4-KO mice indicated that AQP4 is required for RVD (Fig. 1*A*). Astrocytes from WT mice responded to hypo-osmotic stress by a rapid volume increase culminating at ~20 s of hypotonic stress (Fig. 1*B*), followed by a volume decrease reaching basal level at ~150 s of hypotonic stress (Fig. 1*A*). The AQP4-KO astrocytes responded to hypotonic stress by a slower volume increase than in WT (Fig. 1 *A* and *B*). Moreover, knocking out AQP4 abolished RVD and unraveled a volume increase that

Author contributions: V.B., S.F., O.P.O., and M.A.-M. designed research; V.B., M.C., M.D., and M.N.M. performed research; V.B., M.C., and M.A.-M. analyzed data; and V.B., S.F., O.P.O., and M.C. and M.A.-M. wrote the paper.

The authors declare no conflict of interest.

*This Direct Submission article had a prearranged editor.

[1]V.B. and M.C., contributed equally to this work.

[2]To whom correspondence should be addressed. E-mail: mahmo@medisin.uio.no.

This article contains supporting information online at www.pnas.org/lookup/suppl/doi:10.1073/pnas.1012867108/-/DCSupplemental.

reached a steady state at ~100 s and remained at that level through the observation period (Fig. 1*A* and Fig. S1 *A–D*). Preincubation with the intracellular $Ca^{2+}$ chelator 1,2-Bis(2-aminophenoxy)ethane-N,N,N′,N′-tetraacetic acid tetrakis(acetoxymethyl ester (BAPTA-AM) abolished RVD, indicating dependence on $[Ca^{2+}]_i$ (Fig. S1*E*).

Analysis of the $[Ca^{2+}]_i$ response to hypotonic stress in primary WT and AQP4-KO mouse astrocytes and in primary rat astrocytes indicated that AQP4 is required for hypotonicity to elicit an increase in $[Ca^{2+}]_i$ (Fig. 1 *C–F*). The increase in $[Ca^{2+}]_i$ evoked by hypotonic stress reflects $Ca^{2+}$ influx, because it can be abrogated by removal of extracellular calcium $[Ca^{2+}]_o$ (Fig. 1 *C–F*). In addition, stimulation with the TRPV4 agonist 4α-phorbol 12,13-didecanoate (4αPDD) showed that both WT and AQP4-KO astrocytes express functional TRPV4 (Fig. 1 *C–D*). The response to the agonist did not differ significantly between the two types of cell (Fig. 1*F* and Fig. S2 *A–C*).

We have shown previously that rat astrocytes contain functional TRPV4 (8). To demonstrate unequivocally that TRPV4 contributes to hypotonicity-elicited $[Ca^{2+}]_i$ increase and RVD in astrocytes, we knocked down TRPV4 in rat astrocytes using specific siRNA (Fig. 2). Astrocytes were transfected with one of three siRNA oligonucleotides targeting TRPV4 (siRNA 7, 9, or 11) or, alternatively, with Stealth RNAi negative control duplexes (Invitrogen). After 4 d of transfection, Western blot analyses revealed that bands corresponding to specific rat astroglial TRPV4 (8, 10) were attenuated in all siRNA-treated cells compared with control (Fig. 2*A*). The decrease in protein level was more pronounced with siRNA 7 and 9 than with siRNA 11. We selected siRNA 9 for use in the functional analysis because it attenuates all three TRPV4-positive bands (Fig. 2*A*).

Calcium imaging and calcein volume measurements of cells treated with control siRNA or siRNA 9 showed that TRPV4 is necessary for hypotonicity-elicited $[Ca^{2+}]_o$ influx (Fig. 2 *B–D*) and RVD (Fig. 2*E*). These data suggested that AQP4 and TRPV4 are essential for astroglial RVD and that these molecules interact functionally.

We further tested the possibility of a physical interaction between the two molecules. Confocal analysis of triple-labeled rat brain sections showed that TRPV4 and AQP4 colocalize in GFAP-positive processes at the brain surface and in GFAP-positive profiles abutting the extensions of the subarachnoidal space that surround large vessels (Virchow–Robin space) (Fig. 3). Coimmunoprecipitation (co-IP) analyses of whole rat brain extracts indicate that TRPV4 and AQP4 form a molecular complex (Fig. 4 *A* and *B*). TRPV4 does not form complexes with AQP1 (Fig. 4*C*). Immunoprecipitation (IP) of AQP4 with TRPV4 antibodies or IP of TRPV4 with AQP4 antibodies is abolished in AQP4-KO mice, attesting to the specificity of the procedure (Fig. 4 *D* and *E*).

Because TRPV4 has been localized to neurons as well as to astroglial cells (8, 16), it was deemed important to verify that the AQP4–TRPV4 interaction observed in total brain extract also can be demonstrated in primary astrocyte cultures. Our data show that co-IP of TRPV4 and AQP4 can be obtained in extracts of cultured rat astrocytes (Fig. 4 *F* and *G*). No signal was observed when TRPV4 antibody preadsorbed with the immunizing peptide was used for IP (Fig. S3*A*). The TRPV4 pool that is immunoprecipitated by the AQP4 antibody can be subjected to biotinylation, indicating that AQP4 interacts with a plasma membrane pool of TRPV4 (Fig. 4*H*). Thus, after IP with the AQP4 antibody, the TRPV4-immunopositive band comigrates with a biotinylated band (Fig. 4*H*).

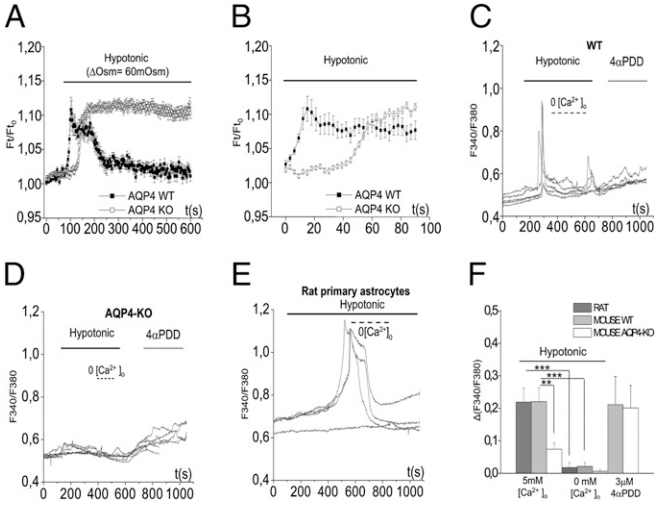


**Fig. 1.** AQP4 is essential for RVD and for the hypotonicity-induced $[Ca^{2+}]_i$ response in primary astroglial cells in primary astroglial cells. (*A*) Calcein-quenching method for measurement of osmotically induced volume changes in primary astroglial cells from WT (closed symbols, $n = 16$) and AQP4-KO mice (open symbols, $n = 30$). The cells were exposed to a hypotonic medium (ΔOsm = 60 mOsm). (*B*) The initial parts of the curves in *A*, shown at higher time resolution. Zero time point on the *x* axis corresponds to 90 s in Fig. 1*A*. Quantitative analyses of data in *A* and *B* are shown in Fig. S1. (*C–E*) Typical $[Ca^{2+}]_i$ dynamics recorded in fura-2–loaded primary astroglial cells from WT mouse (*C*), AQP4-KO mouse (*D*), and rat (*E*). Each line represents the response of an individual cell. (*F*) Quantitative analyses of the hypotonicity-induced $[Ca^{2+}]_i$ response in primary astrocytes. Rat astrocytes ($n = 15$) are shown by the dark gray bar, WT mouse astrocytes ($n = 17$) by the light gray bar, and AQP4-KO astrocytes ($n = 14$) by the white bar. $P = 0.0016$ for the comparison between AQP4 WT and AQP4-KO astrocytes, independent *t*-test; $P < 0.001$ for experiments in presence and absence of $[Ca^{2+}]_o$, paired *t* test. The 4αPDD response did not differ significantly between WT and AQP4-KO cells ($P = 0.9$, independent *t*-test). $^{**}P \le 0.01$; $^{***}P \le 0.001$.

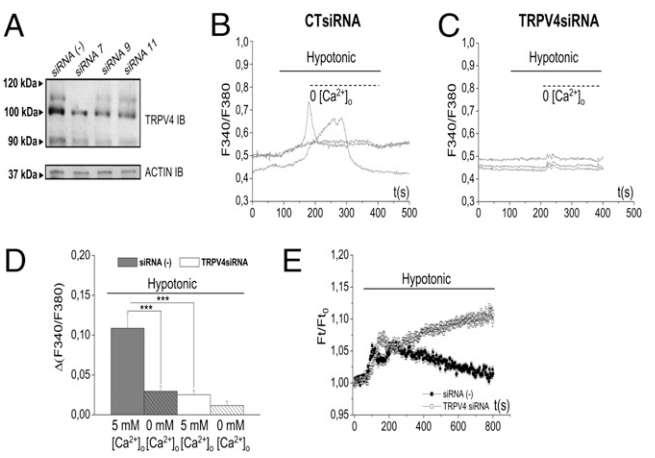


**Fig. 2.** TRPV4 knockdown by siRNA significantly reduces the hypotonicity-induced $[Ca^{2+}]_i$ response and RVD in rat astrocytes. (*A*) The TRPV4 antibody recognizes three major bands of ~90, 100, and 110 kDa. The decrease in TRPV4 protein level, based on densitometric analysis in three different experiments, was most pronounced for siRNA 9 (89% reduction for the 120-kDa band, 61% for the 100-kDa band, and 69% for 90-kDa band) followed by siRNA 7 (89%, 59%, 51%) and siRNA 11 (49%, 54%, 72%). The density of bands of samples treated with control siRNA was set at 100%. The level of actin is not affected by siRNA treatment. (*B*) Typical $[Ca^{2+}]_i$ dynamics recorded in fura-2–loaded primary astroglial cells treated with control (CT) siRNA. (*C*) Knockdown of TRPV4 by siRNA 9 abolishes the $[Ca^{2+}]_i$ response. (*D*) Quantitative analyses of hypotonicity-induced $[Ca^{2+}]_i$ signal in primary astrocytes. Astrocytes treated with CT siRNA ($n = 20$) are shown by the gray bar and astrocytes treated with TRPV4-specific siRNA ($n = 22$) by the white bar. $P < 0.001$ for the comparison between control group and TRPV4 knockdown astrocytes, independent *t*-test; $P < 0.001$ for experiment in presence and absence of $[Ca^{2+}]_o$, paired *t*-test. $^{***}P \le 0.001$. (*E*) Calcein-quenching method for measurement of osmotically induced volume changes in primary astroglial cells treated with control siRNA (closed symbols) and TRPV4-specific siRNA 9 (open symbols). The cells were exposed to a hypotonic medium (ΔOsm = 60 mOsm).

To verify that the AQP4/TRPV4 complex is required for the hypotonicity-induced $[Ca^{2+}]_i$ response and RVD, we performed an analysis of DI TNC1 cells, an astrocyte-derived cell line (17, 18) that expresses GFAP and TRPV4 but not AQP4 (Fig. 4 *I* and *J*). IP experiments showed that the endogenous TRPV4 pool forms complexes with the transfected M1 isoform as well as with the transfected M23 isoform of AQP4 (Fig. 4 *J* and *K*). No complexes were formed when DI TNC1 cells were transfected with AQP1 in lieu of AQP4, attesting to the specific nature of the molecular interaction (Fig. 4*L*).

Complex formation is conserved in different systems and with different recombinant protein species. By cotransfecting recombinant clones of human TRPV4 (hTRPV4)/EGFP and rat AQP4-M1 and AQP4-M23 in COS-7 cells, we verified by co-IP that the two proteins interact (Fig. S3 *B* and *C*). Identical results were obtained when cells were immunoblotted with TRPV4 antibodies in lieu of antibodies to GFP. With the procedures used, coimmunoprecipitation requires that the target and bait molecules actually colocalize, because coimmunoprecipitation could not be demonstrated if AQP4 and TRPV4 were expressed in different populations of cells that were mixed after homogenization (Fig. S3*D*). Moreover, AQP4 was not able to form a complex with cotransfected TRPV1 (Fig. S3*E*), testifying to the binding selectivity of the immunocomplex.

Calcium-imaging analysis showed that nontransfected DI TNC1 cells failed to respond with $[Ca^{2+}]_i$ increase upon hypotonic stress (Fig. 5*A*). Transfection with either isoform of AQP4 confers a hypotonicity-induced $Ca^{2+}$ response on these cells (Fig. 5 *C* and *D*). Transfection of EGFP alone had no effect (Fig. 5*B*). AQP1 could not substitute for AQP4 (Fig. 5*E*, *Inset*). Quantitative analyses of the experiments in Fig. 5 *A*–*D* are shown in Fig. 5*F*.

The increase in $[Ca^{2+}]_i$ evoked by hypotonic stress reflects $Ca^{2+}$ influx, because the increase could be abrogated by removal of $[Ca^{2+}]_o$ (Fig. 5 *C*, *D*, and *F*). In addition, the quantitative analysis showed that the increase in $[Ca^{2+}]_i$ was abolished by gadolinium chloride, supporting the involvement of TRPV channels (Fig. 5*F*).

We then investigated whether the effect of AQP4 transfection on the hypotonicity-induced $Ca^{2+}$ response is mirrored by a corresponding effect on RVD. Transfection of DI TNC1 cells with either isoform of AQP4 or with AQP1 produced a steep increase in initial swelling rate (reflected by the initial slopes in Fig. 6 *A*–*C*), but the absolute volume increase was higher with the AQP4 isoform M1 than with the M23 isoform or with AQP1 (Fig. 6 *A* and *B*). Although nontransfected cells and cells transfected with AQP1 displayed no RVD, both AQP4 transfectants did (Fig. 6 *A* and *D*). Importantly, the magnitude of the RVD response was not significantly different in the two AQP4 transfectants (Fig. 6*D*). Confocal analyses performed on DI TNC1 cells transfected with the M23 isoform of AQP4 or with AQP1 and colabeled with specific antibodies and the plasma-membrane marker wheat germ agglutinin (WGA) revealed that both M23 and AQP1 are trafficked to the plasma membrane (Fig. S4). Thus, the failure of transfected AQP1 to reconstitute a RVD response cannot be explained by intracellular retention of this protein.

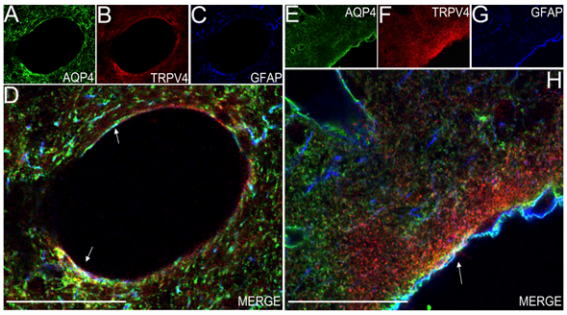


**Fig. 3.** TRPV4 and AQP4 colocalize in astrocytes of adult rat brain. (*A*–*C*) Single-plane confocal immunofluorescence images of large-caliber blood vessel of rat occipital cortex. Triple labeling with goat anti-AQP4 (green, *A*), rabbit anti-TRPV4 (red, *B*), and mouse anti-GFAP (blue, *C*) reveals astrocyte processes that are immunopositive for TRPV4 and AQP4. Triple-labeled processes appear in white in *D*. (Scale bar: 50 μm.) (*E*–*G*) Single-plane confocal immunofluorescence images of sagittal section of rat occipital cortex. Triple labeling with goat anti-AQP4 (green, *E*), rabbit anti-TRPV4 (red, *F*), and mouse anti-GFAP (blue, *G*). Triple-labeled processes appear in white in *H* (merged image, arrow). The triple-labeled processes (white arrows) face the pial surface and surround large-caliber blood vessels. (Scale bars: 50 μm.)

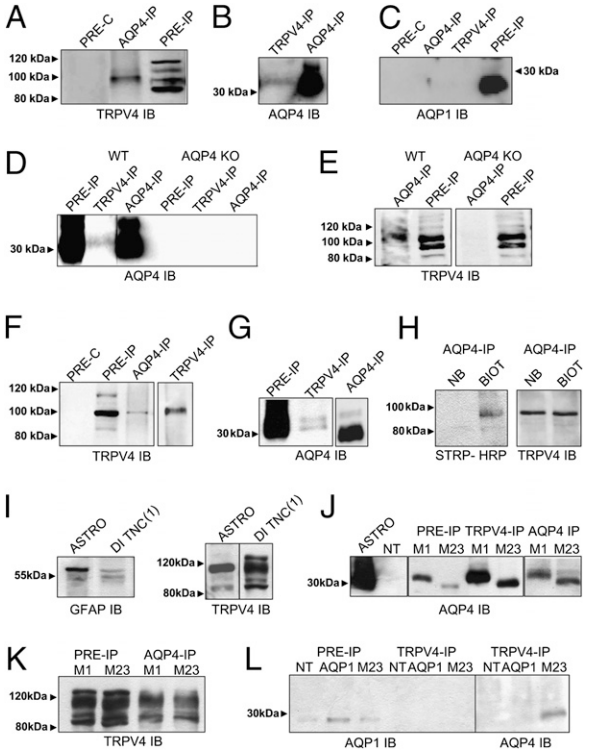


**Fig. 4.** TRPV4 and AQP4 co-IP in rat and mouse brain extracts and in astrocyte-derived cell line DI TNC1. (*A*) Immunoblots of rat brain proteins precipitated by AQP4 antibody show a TRPV4-immunopositive band at the appropriate molecular weight. Omission of AQP4 antibody (Pre-C) abolishes labeling Controls verify the presence of TRPV4-immunopositive bands in brain extract (Pre-IP). (*B*) Same experimental design as in *A*, using TRPV4 antibodies for IP and AQP4 antibodies for immunoblotting. The TRPV4 antibody precipitated an AQP4-immunopositive protein at ~30 kDa. (*C*) Immunoblots of rat brain proteins precipitated by anti-AQP4 or anti-TRPV4 antibody do not show any band positive for AQP1. Control verifies the presence of AQP1 in total brain extract (Pre-IP). (*D*) AQP4-immunopositive band is absent in immunoblots of proteins precipitated by anti-TRPV4 or anti-AQP4 from brains of AQP4-KO mice. (*E*) The same experimental design as in *D*, using TRPV4 antibody for immunoblotting. Knockout of AQP4 abolishes the ability of anti-AQP4 to precipitate TRPV4. (*F* and *G*) TRPV4 can be immunoprecipitated by AQP4 antibodies (*F*) and vice versa (*G*) in primary astroglial cultures. (*H*) IP experiments on primary astrocytes treated with biotin to label membrane proteins. The AQP4 antibody pulls down a biotinylated protein (BIOT), identified by streptavidin-HRP (STRP-HRP, *Left*). This protein comigrates with the band immunopositive for TRPV4 (*Right*). NB, nonbiotinylated sample. (*I*–*L*) An AQP4/TRPV4 complex can be reconstituted in the astrocyte-derived cell line DI TNC1. (*I*) Immunoblots showing that DI TNC1 cells express GFAP (*Left*) and TRPV4 (*Right*). Primary astrocytes (ASTRO) are used for reference. (*J*) AQP4 is not expressed in nontransfected (NT) DI TNC1 cells. Transfected M1 and M23 AQP4 isoforms are precipitated by TRPV4 antibodies. Pre-IP, total cell lysate. (*K*) Endogenous TRPV4 is precipitated by AQP4 antibodies in cells transfected with M1 or M23 AQP4 isoforms. (*L*) Overexpression of AQP1 induced an increased signal at the appropriate molecular weight only in AQP1-transfected DI TNC1 cells. Note that AQP1 is not precipitated by endogenous TRPV4.

## Discussion

RVD is a basic cell biological response and an important element in the cell's defense reaction to the challenges imposed by hypo-osmotic stress (1). Because osmotic stress is a prevalent form of stress even in eukaryotic organisms with a well-controlled *milieu interne*, the ability to readjust cell volume is a property common to most mammalian cells. However, the efficiency of RVD and hence also its molecular underpinning vary among organs and cell populations (1, 9, 14). Astroglial cells are known to show a brisk RVD response as judged by analyses of isolated cells as well as astrocytes in situ (6, 19, 20).

A hallmark of RVD in astrocytes and other cells is activation of VRAC that mediates an efflux of inorganic osmolytes. This efflux provides a driving force for outward water transport (6–8, 20). The upstream mechanisms have remained obscure. Thus, there is a remarkable void in our knowledge of how volume homeostasis is maintained either at the cellular level or in the brain as a whole.

By definition, an RVD response is set in motion by a decrease in external osmolarity (1). This decrease must be sensed by the cells, either directly, or indirectly, by way of the consequent cell-volume increase. In astroglia there is evidence indicating that an increase in $[Ca^{2+}]_i$ plays a pivotal role (1, 20, 21). TRPV4 is endowed with properties that make it a likely candidate for an astroglial osmo-sensor (22). This polymodal channel responds to mechanical stress by mediating $Ca^{2+}$ influx, raising the possibility that TRPV4 may be fully or partly responsible for the $[Ca^{2+}]_i$ increase that triggers RVD (22). In a human keratinocyte cell line and in CHO cells, TRPV4 was shown to be involved in RVD (9, 23). The same studies demonstrated that TRPV4 per se is not sufficient and that its interaction with the actin cytoskeleton is critical for triggering RVD (23).

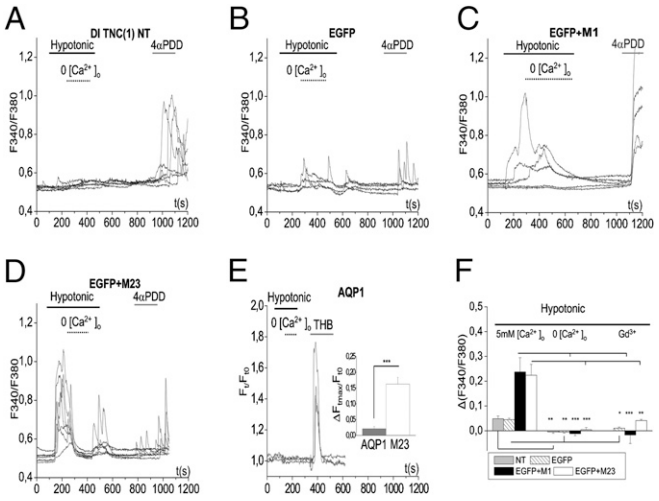


**Fig. 5.** Hypotonicity-induced $Ca^{2+}$ response is reconstituted in AQP4 (M1 or M23)-transfected but not in AQP1-transfected DI TNC1 cells. (*A*) Traces representative of typical variations in $[Ca^{2+}]_i$ observed in fura-2–loaded DI TNC1 nontransfected (NT) cells exposed to hypotonic solution (black bar; ΔOsm = 60 mOsm) in the presence or absence of 5 mM $[Ca^{2+}]_o$ (hatched bar) and stimulated with 5 μM 4αPDD (gray line). (*B–D*) Representative traces depicting $[Ca^{2+}]_i$ DI TNC1 cells transfected with EGFP (*B*), EGFP + M1 (*C*), or EGFP + M23 (*D*). The experimental design is as in *A*. (*E*) Typical $Ca^{2+}$ dynamics of three Fluo-4-AM–loaded DI TNC1 cells transfected with AQP1 showing no $[Ca^{2+}]_i$ signal upon hypotonicity. Thrombine (10 μM; THB; gray line) was used as positive control. (*Inset*) Quantitative analyses of maximal variation in fluorescence ratio (Δ*F*/*F*) recorded in AQP1 (gray bar; *n* = 16) and AQP4-M23 (*n* = 6) transfected cells upon cell exposure to hypotonic solution. (*F*) Quantitative analysis of data represented in *A–D*. Mean of variation in fluorescence ratio (Δ*F*340/*F*380) recorded upon cell exposure to hypotonic solution in presence (*Left*) or in absence (*Center*) of $[Ca^{2+}]_o$ (NT, nontransfected, light gray bar, *n* = 36; EGFP, hatched bar, *n* = 32; AQP4-M1, black bar, *n* = 19; AQP4-M23, white bar, *n* = 13) (ANOVA and post hoc, independent *t*-test $P < 0.001$ for AQP4-M1/NT-EGFP and AQP4-M23/NT-EGFP).The increase is abolished in absence of $[Ca^{2+}]_o$. The histogram also includes data obtained by adding gadolinium chloride ($Gd^{3+}$) to the hypotonic saline to block TRPV cation channels (*Right*). The application of $Gd^{3+}$ abolished the $[Ca^{2+}]_i$ signal. (paired *t*-test, $P < 0.001$ for analyses in presence and absence of $[Ca^{2+}]_o$; independent *t*-test for experiment with $Gd^{3+}$, $P = 0.004$ in AQP4-M1 cells, $n = 10$; $P < 0.001$ in AQP4-M23 cells, $n = 16$; $P < 0.05$ in EGFP cells, $n = 6$). $P \le 0.05$; $^{**}P \le 0.01$; $^{***}P \le 0.001$.

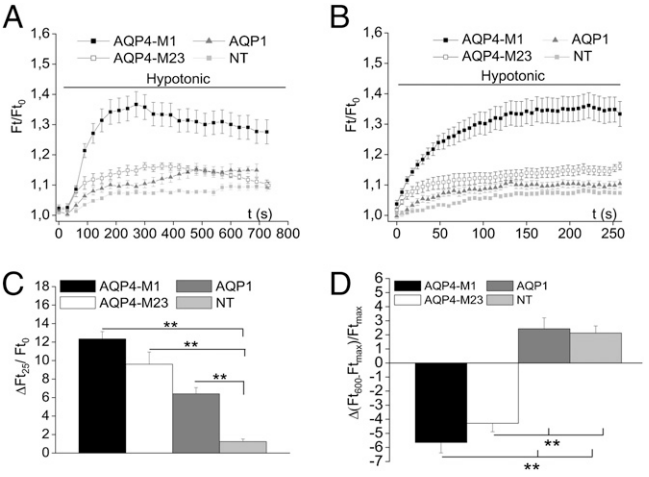


**Fig. 6.** Transfection with M1 or M23 isoforms of AQP4 reconstitutes hypotonicity-induced RVD in DI TNC1 cells. (*A*) Calcein-quenching method for measurement of osmotically-induced volume changes in cells transfected with AQP4-M1 (black, *n* = 15), AQP4-M23 (white, *n* = 22), or AQP1 (gray, *n* = 17) and in nontransfected cells treated with Lipofectamine only (NT; light gray, *n* = 46). (*B*) Direct comparison of the initial phase (the first 200 s following exposure to hypotonic medium) of curves depicted in *A*. The initial swelling is significantly faster in all the transfected cells than in the non-transfected cells. (*C*) Quantitative analysis of data presented in *A*. Ordinate values represent mean rate of volume change at 25 s of hypotonic stress compared with baseline level. ($P > 0.001$; ANOVA and independent *t*-test, *n* as in *A*). No significant difference is detectable between cells transfected with AQP4-M1 (black; *n* = 15) and cells transfected with AQP4-M23 (white; *n* = 22; $P = 0.135$; independent *t*-test). $^{**}P \le 0.01$. (*D*) Ordinate values represent mean volume change calculated as described in *Materials and Methods*. A decrease in regulatory volume, represented by negative values, is seen after transfection with AQP4 isoforms M1 (black bar) or M23 (white bar) but not after transfection with AQP1 cells (dark gray bar) or in nontransfected (NT) cells (light gray bar). $P < 0.01$; ANOVA and independent *t*-test. $^{**}P \le 0.01$.

Our recent demonstration (8) of a TRPV4 pool in astroglial membranes at the brain surface, in close apposition to the subarachnoid space, led us to propose that TRPV4 is engaged in RVD processes that could serve to regulate the volume of astrocyte syncytia and hence contribute significantly to volume regulation of the brain as a whole.

We also noted (8) that the distribution of TRPV4 in subpial and subependymal glial membranes mimics that of AQP4, the predominant water channel in brain (3). The present study was initiated to explore the roles of AQP4 and TRPV4 in RVD and to test whether there is a physical and functional interaction between these two molecules.

Here we show that primary astrocytes lose their ability to sustain RVD after AQP4 depletion. A salient observation is that depletion of AQP4 also abolishes the $[Ca^{2+}]_i$ increase normally seen in response to hypotonic stress. Because AQP4 is impermeant to $Ca^{2+}$, this finding provided a clue that AQP4 interacts with an osmosensitive $Ca^{2+}$ channel.

We hypothesized that the $Ca^{2+}$ channel in question was identical to TRPV4. Supporting this idea, we found that siRNA knockdown of TRPV4 caused a pronounced reduction in the $Ca^{2+}$ response to hypo-osmotic stress and also abolished RVD. Thus, our data were consistent with the idea that both molecules are indispensable for eliciting downstream effects of hypo-osmotic

stress. In the siRNA knockdown experiments the effect on TRPV4 expression (Fig. 2*A*) was on a par with the effect on hypotonicity-induced $[Ca^{2+}]_i$ response (Fig. 2*D*).

By a combination of immunocytochemistry and co-IP techniques, we were able to provide evidence that AQP4 and TRPV4 colocalize and interact physically in situ as well as in primary cortical astrocytes in culture. Different in vitro approaches then were undertaken to characterize the functional interaction of the two molecules.

To test if TRPV4 and AQP4 interaction triggers RVD, we took advantage of DI TNC1 cells which are derived from astroglia (17, 18). Because these cells lack endogenous AQP4 (but express endogenous TRPV4), they offer a unique model system to resolve how astroglial RVD depends on the AQP4/TRPV4 complex. In DI TNC1 cells that were not transfected with AQP4, hypotonic stress failed to induce $[Ca^{2+}]_i$ increase and RVD response. However, both the $Ca^{2+}$ response and RVD were reconstituted in these cells by transfection with AQP4.

In sum, our data suggest that AQP4 and TRPV4 are essential components of a molecular complex that initiates RVD in astrocytes.

The first issue to be discussed relates to the molecular specificity. In other words, is there promiscuity in the system so that TRPV4 also could initiate RVD when partnered with an aquaporin other than AQP4? Or, vice versa, could AQP4 bind to another member of the TRPV family? Our data show that TRPV4 fails to precipitate AQP1 from brain extracts and in a transfected astroglial cell line. Previous studies have shown an interaction between aquaporin-5 (AQP5) and TRPV4 in salivary glands (11, 12). It well may be that in these glands a TRPV4/AQP5 complex plays a role analogous to that of the TRPV4/AQP4 complex in brain. AQP5 has not been demonstrated in astrocytes. In fact, AQP4 is the only AQP that is enriched in endfeet, suggesting that AQP4 is the sole AQP binding partner for TRPV4 in situ.

That another member of the TRPV family could replace TRPV4 as an AQP4 binding partner is unlikely also. The IP experiments show that AQP4 is unable to bind TRPV1. The latter has been suggested to act in concert with TRPV4 in osmotransduction and systemic control of anisotonicity (22, 24). TRPV2 is the only other TRPV family member that is expressed in brain and shares the osmo- and mechanosensitive properties of TRPV4 and TRPV1 (14, 15, 24, 25). However, TRPV2 is not functional in cultured astrocytes (8).

How do AQP4 and TRPV4 interact? Our analysis shows that the two molecules must be present in the same cells (and not just in the same extract) to be subject to IP. This result implies that IP in our setting reflects real interaction—direct or through intervening proteins—and not merely an ability to interact. It should be emphasized that all IP experiments were conducted in the absence of chemical cross-linkers. The specific amino acid sequences that are crucial for complex formation will have to be resolved in further studies. However, it is clear that the N-terminal 22 amino acids of the AQP4 M1 isoform are not involved, because IP of TRPV4 also was observed with the M23 isoform.

We detected only one TRPV4-positive band of ~100 kDa after AQP4 IP of mouse or rat brain extracts (Fig. 4 *A* and *F*). This result suggests that there is isoform selectivity in the interaction between AQP4 and TRPV4. The most parsimonious explanation of this selectivity is that TRPV4 isoforms (26) differ in their trafficking to the plasma membrane (27). In agreement, our biotinylation experiment (Fig. 4*H*) revealed a single biotinylated band in the MW range of known TRPV4 isoforms.

Given a direct physical interaction between TRPV4 and AQP4, the possibility remains that AQP4 serves merely to allow water influx, and that TRPV4 is activated by the consequent volume increase and membrane stretch.

In opposition to this rather trivial explanation, we found that AQP1 could not substitute for AQP4 in promoting hypotonicity-induced $[Ca^{2+}]_i$ elevation or RVD. AQP1 and AQP4 show similar water-fluxing capacities (18). Taken together, our findings indicate that physical interaction of AQP4 with TRPV4 is essential for TRPV4 to function as an astroglial osmosensor.

Reflecting its critical importance for cell survival, volume regulation is served by a multitude of mechanisms that differ in various cells and organs. This heterogeneity calls for caution in generalizing from the present data. Because TRPV4 is enriched mainly in superficial astroglia, its role in volume regulation is likely to be particularly important for the astrocytic syncytia that abut on the subarachnoidal and perivascular spaces. Export of osmolytes to the cerebrospinal fluid is an essential element of the brain's response to acute hypo-osmotic stress, and our data are consistent with the idea that the TRPV4/AQP4 complex contributes to this response. In contrast, endfeet surrounding brain microvessels show a strong AQP4 immunosignal (3) but only a weak TRPV4 immunosignal (8), suggesting that the perivascular pool of AQP4, which serves as an influx route for water under pathophysiological conditions, is not involved in TRPV4-dependent volume regulation. This dual expression pattern would explain why there is a net protective effect of knocking out AQP4 in conditions that favor build up of brain edema (28).

## Conclusion

In our previous study we showed that cultured astrocytes exhibit a rise in $[Ca^{2+}]_i$ in response to hypo-osmotic stress and presented pharmacological data pointing to the involvement of TRPV4 in this $[Ca^{2+}]_i$ increase (8). Here we have shown that the $[Ca^{2+}]_i$ increase and volume response to hypotonic stress can be reconstituted in cells that coexpress TRPV4 and AQP4. These data support the idea that TRPV4 and AQP4 are instrumental in triggering astroglial RVD and that the two molecules must be coexpressed for astroglial RVD to occur. The dissection of the molecular underpinning of astroglial volume homeostasis could open approaches for therapy in conditions of deranged water transport or distribution.

## Materials and Methods

**Animals.** Experiments on animals were performed according to the European Council law on protection of laboratory animals, with the approval of a local bioethics committee and under the supervision of a veterinary commission for animal care and comfort of the University of Bologna and the University of Oslo. Every effort was made to minimize the number of animals used and their suffering.

**Plasmids and Antibodies.** The human TRPV1 (hTRPV4)/pEGFP-N1 and TRPV1/pEYFP constructs were a gift from Antonio Ferrer-Montiel (8). The AQP4-M1 and AQP4-M23 constructs encoding for the two isoforms of AQP4 mainly expressed in astrocytes (3) were a gift from Anita Aperia (Karolinska Institute, Stockholm, Sweden) (29). The following antibodies were used: rabbit anti-TRPV4 (Alomone), mouse anti-AQP1 (Abcam), mouse anti-GFP (Roche), goat anti-AQP4 (Santa Cruz), rabbit anti-TRPV1 (a gift from Antonio Ferrer-Montiel, Instituto de Biologia Molecular y Celular, Universidad Miguel Hernández, Elche, Spain), and mouse anti-GFAP (Chemicon). Preadsorbtions with immunizing peptides were performed as controls.

**siRNA and Transfection.** Stealth RNAi siRNA select RNAi (a set of three oligos: ID RSS330372, designated " number 7"; ID RSS330373, designated "number 9"; and ID RSS330374, designated "number 11") which respectively target nucleotides 1322–1346, 1201–1225, and 1642–1666 of rat TRPV4 (GenBank accession no. NM_023970.1) were purchased from Invitrogen. Transfection was performed on 2- to 3-wk-old primary astrocytes using Lipofectamine RNAiMAX and Opti-MEM I reduced serum medium according to the manufacturer's instructions (Invitrogen). A more detailed description of the procedure is given in *SI Materials and Methods*.

**Immunofluorescence.** Wistar male rats (8–10 wk old) were perfusion-fixed, and the tissue was processed for immunofluorescence as previously described (8, 30). Immunostaining was performed on brain sections (thickness 15–20 μm) following protocols previously described (8). For immunodetection, secondary antibodies used were Alexa Fluor 488-conjugated donkey anti-goat, Alexa Fluor 595 donkey anti-rabbit, and Cy5 donkey anti-mouse. Images of rat brain sections were captured using a Zeiss SP1/MP confocal microscope and processed using Zeiss Imaging software. Preadsorption controls were performed according to the manufacturer's instructions. Immunofluorescence on DI TNC1 with Alexa Fluor 488 was performed following protocols previously described (8).

**Cell Culture and Transfection.** Primary cultured rat cortical astrocytes were prepared, and DI TNC1 cells were cultured and maintained as described previously (31).

DI TNC1 cells were transfected with the pEGFP-N1 construct or cotransfected with pEGFP-N1 + AQP4-M1 or + AQP4-M23 by use of Lipofectamine 2000, following the manufacturer's instructions (Invitrogen). All experiments on transfected cells were performed 48 h after transfection.

**Biotinylation of Cell-Surface Membrane Protein.** Biotinylation of cell-surface membrane proteins was performed on cultured astrocytes as previously described (31). To test the specificity of the assay, the same experiment was performed without the addition of biotin donor. IP experiments were performed on equal amounts of total protein of biotinylated and nonbiotinylated samples (7, 8).

**Immunoprecipitation.** Eight- to ten-week-old Wistar rats and 4-wk-old male AQP4-WT mice andAQP4-KO mice generated in a C57Bl6/J background were used for these studies. Rodent brain tissues were homogenized, and whole-protein extracts (preimmunoprecipitation product, pre-IP) were obtained as previously described (8). Cultured astrocytes and nontransfected and transfected COS-7 and DI TNC1 cells were harvested in the lysis buffer, scraped off, and protein was extracted as previously described (7, 8). The IP that was obtained by incubating pre-IP with rabbit anti-TRPV4 or mouse anti-AQP4 antibodies (10 μg Ab/0.500 mg of whole-protein lysates) at 4 °C overnight. Immunocomplexes were captured with protein A Sepharose (50 μL; Amersham), washed at least seven times with 500 μL washing buffer at 4 °C, dissociated with 75 μL Laemmli sample buffer, warmed for 30 min at 37 °C, and analyzed by SDS/PAGE and immunoblotting. To test unspecific binding of protein A Sepharose, the assay was performed in the absence of primary antibody (precleaning, pre-C).

**Immunoblotting.** SDS/PAGE and Western blot analyses were performed as described previously (7, 8). Briefly, whole-protein extracts (pre-IP), 50 μL IP, and 50 μL Pre-C samples were separated by 7.5% or 12% SDS/PAGE and electrotransferred onto nitrocellulose membranes (Bio-Rad Laboratories). Blots were incubated with primary antibody (see *Plasmids and Antibodies*) and HRP-conjugated secondary antibody (Sigma) or with HRP-conjugated streptavidin (1:2,000; Dako), diluted in blocking solution (8). Immunoreactive bands were visualized using ECL-Plus (Amersham Biosciences). Densitometry of the signal was performed by using the Aida Image Analyzer (Raytest).

**Calcium Microfluorometry.** Changes in $[Ca^{2+}]_i$ concentration were measured at room temperature (22 °C) by ratiometric microfluorometry using the fluorescent $Ca^{2+}$ indicator fura-2-acetoxymethyl ester (fura-2-AM) (Molecular Probes, Invitrogen) following procedures and protocols described previously (8). Details are given in *SI Materials and Methods*.

**Water Permeability and Cell-Volume Measurements.** Cell-volume changes in nontransfected cells and in cells transfected with AQP4-M1, AQP4-M23, or AQP1 were analyzed by the calcein-quenching fluorescence method. For detailed procedures, see *SI Materials and Methods*.

**Solutions and Chemicals.** Salts and other chemicals were of the highest purity grade (Sigma-Aldrich). For microfluorometric experiments the standard bath saline, the extracellular isotonic saline, and hypotonic saline were prepared as previously described (8). Aliquots of 4αPDD were prepared by dissolving it in DMSO 500-fold more concentrated than the final dilution and kept at −20 °C. Stock solutions (10 mM) of gadolinium were prepared in water, and aliquots were kept at −20 °C.

**Statistics.** All data are expressed as means of several cells ($n$) ± SEM. The statistical evaluation was performed with ANOVA post hoc or student's $t$-test performed with Microcal Origin. A $P$ value $< 0.05$ was considered statistically significant.

**ACKNOWLEDGMENTS.** We thank Vittorio Vellani for assistance in fluo-4 $Ca^{2+}$ imaging and Laura Giardini for technical assistance, Paola Nicchia, University of Bari, Italy, for the AQP1, Anita Aperia, Karolinska Institute, Stockholm, Sweden, for the AQP4 M1 and AQP4-M23 clones, Prof. Antonio Ferrer-Montiel for providing the hTRPV4/pEGFP-N1 and TRPV1/pEYFP constructs and anti-TRPV1 antibody, and Laura Camassa and Alessia Minardi for their assistance in astrocyte preparation. This work was supported by a grant from the Research Council of Norway (to M.A.-M. and O.P.O.), by European Molecular Biology Organization short-term Fellowship ASTF89-2007, and by a postdoctoral Fellowship from the University of Bologna (to V.B.) and from Progetti Strategici di Ateneo 2007, University of Bologna (to M.C.). Additional funding was obtained from EU projects PF6 035859-2 (BIMORE) and FP7-ICT- 248052 (PHOTO-FET), and Italian Minister for University FIRBRBPR05JH2 (Italnanonet).

1. Pasantes-Morales H, Lezama R-A, Ramos-Mandujano G, Tuz K-L (2006) Mechanisms of cell volume regulation in hypo-osmolality. *Am J Med* 119(7, Suppl 1)S4–S11.
2. Simard M, Nedergaard M (2004) The neurobiology of glia in the context of water and ion homeostasis. *Neuroscience* 129:877–896.
3. Amiry-Moghaddam M, Ottersen O-P (2003) The molecular basis of water transport in the brain. *Nat Rev Neurosci* 4:991–1001.
4. Verbalis J-G (2006) Control of brain volume during hypoosmolality and hyperosmolality. *Adv Exp Med Biol* 576:113–129, discussion 361–363.
5. Amiry-Moghaddam M, Frydenlund D-S, Ottersen O-P (2004) Anchoring of aquaporin-4 in brain: Molecular mechanisms and implications for the physiology and pathophysiology of water transport. *Neuroscience* 129:999–1010.
6. Kimelberg H-K (2005) Astrocytic swelling in cerebral ischemia as a possible cause of injury and target for therapy. *Glia* 50:389–397.
7. Benfenati V, et al. (2007) Functional down-regulation of volume-regulated anion channels in AQP4 knockdown cultured rat cortical astrocytes. *J Neurochem* 100:87–104.
8. Benfenati V, et al. (2007) Expression and functional characterization of transient receptor potential vanilloid-related channel 4 (TRPV4) in rat cortical astrocytes. *Neuroscience* 148:876–892.
9. Becker D, Blase C, Bereiter-Hahn J, Jendrach M (2005) TRPV4 exhibits a functional role in cell-volume regulation. *J Cell Sci* 118:2435–2440.
10. Arniges M, Vázquez E, Fernández-Fernández J-M, Valverde M-A (2004) Swelling-activated Ca2+ entry via TRPV4 channel is defective in cystic fibrosis airway epithelia. *J Biol Chem* 279:54062–54068.
11. Liu X, et al. (2006) A role for AQP5 in activation of TRPV4 by hypotonicity: Concerted involvement of AQP5 and TRPV4 in regulation of cell volume recovery. *J Biol Chem* 281:15485–15495.
12. Sidhaye V-K, et al. (2006) Transient receptor potential vanilloid 4 regulates aquaporin-5 abundance under hypotonic conditions. *Proc Natl Acad Sci USA* 103:4747–4752.
13. Pan Z, et al. (2008) Dependence of regulatory volume decrease on transient receptor potential vanilloid 4 (TRPV4) expression in human corneal epithelial cells. *Cell Calcium* 44:374–385.
14. Liedtke W (2008) Molecular mechanisms of TRPV4-mediated neural signaling. *Ann N Y Acad Sci* 1144:42–52.
15. Mutai H, Heller S (2003) Vertebrate and invertebrate TRPV-like mechanoreceptors. *Cell Calcium* 33:471–478.
16. Liedtke W, et al. (2000) Vanilloid receptor-related osmotically activated channel (VR-OAC), a candidate vertebrate osmoreceptor. *Cell* 103:525–535.
17. Radany E-H, et al. (1992) Directed establishment of rat brain cell lines with the phenotypic characteristics of type 1 astrocytes. *Proc Natl Acad Sci USA* 89:6467–6471.
18. Mola M-G, Nicchia G-P, Svelto M, Spray D-C, Frigeri A (2009) Automated cell-based assay for screening of aquaporin inhibitors. *Anal Chem* 81:8219–8229.
19. Chvátal A, Anderová M, Kirchhoff F (2007) Three-dimensional confocal morphometry - a new approach for studying dynamic changes in cell morphology in brain slices. *J Anat* 210:671–683.
20. Mongin A-A, Cai Z, Kimelberg H-K (1999) Volume-dependent taurine release from cultured astrocytes requires permissive [Ca(2+)](i) and calmodulin. *Am J Physiol* 277:C823–C832.
21. O'Connor E-R, Kimelberg H-K (1993) Role of calcium in astrocyte volume regulation and in the release of ions and amino acids. *J Neurosci* 13:2638–2650.
22. Liedtke W (2006) Transient receptor potential vanilloid channels functioning in transduction of osmotic stimuli. *J Endocrinol* 191:515–523.
23. Becker D, Bereiter-Hahn J, Jendrach M (2009) Functional interaction of the cation channel transient receptor potential vanilloid 4 (TRPV4) and actin in volume regulation. *Eur J Cell Biol* 88:141–152.
24. Cohen D-M (2007) The transient receptor potential vanilloid-responsive 1 and 4 cation channels: Role in neuronal osmosensing and renal physiology. *Curr Opin Nephrol Hypertens* 16:451–458.
25. Liapi A, Wood J-N (2005) Extensive co-localization and heteromultimer formation of the vanilloid receptor-like protein TRPV2 and the capsaicin receptor TRPV1 in the adult rat cerebral cortex. *Eur J Neurosci* 22:825–834.
26. Arniges M, Fernández-Fernández JM, Albrecht N, Schaefer M, Valverde MA (2006) Human TRPV4 channel splice variants revealed a key role of ankyrin domains in multimerization and trafficking. *J Biol Chem* 281(3):1580–1586.
27. Cohen D-M (2006) Regulation of TRP channels by N-linked glycosylation. *Semin Cell Dev Biol* 17:630–637.
28. Zeynalov E, et al. (2008) The perivascular pool of aquaporin-4 mediates the effect of osmotherapy in postischemic cerebral edema. *Crit Care Med* 36:2634–2640.
29. Zelenin S, Gunnarson E, Alikina T, Bondar A, Aperia A (2000) Identification of a new form of AQP4 mRNA that is developmentally expressed in mouse brain. *Pediatr Res* 48:335–339.
30. Amiry-Moghaddam M, et al. (2004) Alpha-syntrophin deletion removes the perivascular but not endothelial pool of aquaporin-4 at the blood-brain barrier and delays the development of brain edema in an experimental model of acute hyponatremia. *FASEB J* 18:542–544.
31. Benfenati V, Caprini M, Nobile M, Rapisarda C, Ferroni S (2006) Guanosine promotes the up-regulation of inward rectifier potassium current mediated by Kir4.1 in cultured rat cortical astrocytes. *J Neurochem* 98:430–445.